Photoprotection of *Punica granatum* seed oil nanoemulsion entrapping polyphenol-rich ethyl acetate fraction against UVB-induced DNA damage in keratinocytes HaCat cell line

Thaisa Baccarin[a,c], Montserrat Mitjans[a], David Ramos[b], Joaquín de la Puente[b], Elenara Lemos-Senna[c], Maria Pilar Vinardell[a*]

[a]Departament de Fisiologia, Facultat de Farmàcia, Universitat de Barcelona, Barcelona, Spain, [b] Unidad de Toxicología y Ecotoxicología del Parc Cientific de Barcelona, Barcelona, Spain

[c]Programa de Pós-Graduação em Farmácia, Universidade Federal de Santa Catarina, 88040-900, Florianópolis, Brazil.

*Corresponding author: mpvinardellmh@ub.edu. Departament de Fisiologia, Facultat de Farmàcia, Universitat de Barcelona, Av. Joan XXIII s/n, E-08028 Barcelona, Spain. Tel.: +34 934024505; fax: +34 934035901.

Abstract

There has been an increase in use of botanicals as skin photoprotective agents. Pomegranate (*Punica granatum* L.) is well known for the high concentration of polyphenolics compounds and for the antioxidant and antiinflamatory properties. The aim of this study was to analyse the photoprotection of *Punica granatum* seed oil nanoemulsion entrapping polyphenol-rich ethyl acetate fraction against UVB-induced DNA damage in keratinocytes HaCat cell line. For this purpose, HaCaT cells were pretreated for 1 h with nanoemulsions in a serum-free medium and then irradiated with

UVB (90–200 mJ/cm^2) rays. Fluorescence microscopy analysis provided information about the cell internalization of the nanodroplets. We also determined the *in vitro* SPF of the nanoemulsions and evaluated the phototoxicity assessed by 3T3 Neutral Red Uptake Phototoxicity Test. The nanoemulsions were able to protect the cell DNA against UVB-induced damage in a concentration dependent manner. Nanodroplets were internalized by the cells but a greater amount was detected along the cell membrane. The higher SPF obtained (~25) depended on the concentration of the ethyl acetate fraction and pomegranate seed oil in the nanoemulsions. The formulations were classified as non-phototoxic (1<PIF<2). Finally, nanoemulsions entrapping polyphenol-rich ethyl acetate fraction exhibited a potential application as a sunscreen product.

Keywords: *Punica granatum*, pomegranate seed oil, cytotoxicity, phototoxicity, cell internalization, photoprotection.

1. Introduction

The ultraviolet radiation (UVR) is a very important exogenous factor in skin pathogenesis and can lead to the development of a number of skin disorders including sunburn, immunosuppression, carcinogenesis, and photoaging. The UVR can be divided in three regions: ultraviolet C (UVC – from 200 to 290 nm); ultraviolet B (UVB - from 290 to 320 nm) and ultraviolet A (UVA - from 320 to 400 nm) [1]. UVC radiation is filtered by the ozone layer before reaching the earth. UVA is the most responsible radiation for the photoaging; it penetrates deeper into de epidermis and dermis of the skin and is barely able to excite the DNA molecule directly, therefore, it is assumed that much of the mutagenic and carcinogenic action is mediated through oxidative stress [1]. UVB radiation (290-320 nm) is responsible for the damage due to sunburn (erythema and edema), induction of oxidative stress, and is a very genotoxic agent. Direct absorption of

UVB photons leads to disruption of DNA, with cyclobutane-pyrimidine dimers (CPD) and pyrimidine-pyrimidone (6-4) photoproducts as a result, which, if remain unrepaired can iniciate photocarcinogenesis. It is less penetrating than UVA, mostly only reaches the epidermal basal cell layer of the skin and thus affects mainly epidermal cells, possibly altering the proliferation, differentiation and metabolism of these cells [2-4].

Thus, protection of skin against excessive sunlight exposure is essential to forestall the damage. Exogenous application of protective dermatological preparations containing sunscreens (organic and/or inorganic filters) is commonly recommended. In this regard, naturally occurring plant products have also been investigated and play a role in a broad range of physiological processes including protection against harmful UVR. Due to the sunscreen effect, potent antioxidant, antiinflamatory and immunomodulatory properties, polyphenols are among the most promising group of compounds that can be exploited as ideal chemopreventive agents for a variety of skin disorders [1, 3].

Punica granatum (pomegranate) is an ancient fruit, considered as "a pharmacy unto itself" with enormous health benefits [5-7]. The main compounds responsible for most of the functional properties are phenolic compounds. They can be found in substantial amounts and in different parts of the fruit (bark, flower, leaves, arils) but are much more concentrated on the peel and juice. The peel is rich in hydrolysable tannins, mainly punicalin, peduncalagin and punicalagin; hydroxybenzoic acids such gallic acid and ellagic acid; anthocyanidins and flavonoids. They account for 92% of the antioxidant activity associated with the fruit [8]. The pomegranate seed oil contains a phytosterols, tocopherols and a unique fatty acid composition, mainly consisting of punicic acid (50-70 %), which is considered as one of the strongest natural antioxidants [9].

Recently we developed pomegranante seed oil nanoemulsions (PSO-NE) and medium chain triglyceride nanoemulsions (MCT-NE) both of them entrapping a

pomegranate peel polyphenol-rich ethyl acetate fraction (EAF) for topical administration and evaluated the antioxidant activity by *in vitro* methods (Article accepted). Nanoemulsions (NE) present large surface area and low surface tension of the oil droplets which could be an advantage to increase the permeation of the incorporated polyphenol compounds through the skin, enhancing the topical effect [10-12]. In another previous work erythrocyte-based assays were employed to verify if EAF-loaded NE could protect the membrane lipid bilayer against the oxidative stress induced by oxidant agents since erythrocytes are well known as a biomembrane model that mimic a cellular environment, and also to verify if any nanoemulsion component (mainly surfactants) could possibly damage the cell membrane and lead to hemolysis (Article submmited).

The main purpose of this study was to investigate whether the free EAF and EAF-loaded nanoemulsions can exert photoprotective effect against DNA damage induced by UVB irradiation, assessed on monolayers cultures of human keratinocytes HaCat as well as to determine the cytotoxicity and phototoxicity of the formulations. Finally, cell internalization studies were conducted to predict the possible localization of the nanoemulsion when in contact with cell.

2. Materials and Methods

2.1 Materials

Polysorbate (Tween 80®), triethanolamine, dimethyl sulfoxide (DMSO), 2,5 diphenyl-3,-(4,5-dimethyl-2-thiazolyl) tetrazolium bromide (MTT), neutral red dye, nile red (NR), calcein and 4,6 diamino-2-phelylindole dihydrochloride hydrate (DAPI) were purchased from Sigma-Aldrich (St. Louis, MO, USA). NaCl, Na_2HPO_4 and KH_2PO_4 were purchased from Merck (Darmstadt, Germany). Sodium acetate, ethyl acetate, dichloromethane,

chloride acid, ethanol were obtained from Vetec® (Rio de Janeiro, Brazil). Pomegranate seed oil and pomegranate fruit peel dry extract were purchased from Via Farma (São Paulo, Brazil). Soy lecithin (Lipoid® S100) was from Lipoid AG (Steinhausen, Switzerland). Medium chain triglyceride was from Brasquim (Porto Alegre, Brazil) and water was purified in a Milli-Q system (Millipore, Bedford, MA). Dulbecco's modified Eagle's medium (DMEM), fetal bovine serum (FBS), phosphate buffered saline (PBS), L-glutamine solution (200 mM), trypsin–EDTA solution (170,000 U/L trypsin and 0.2 g/L EDTA) and penicillin–streptomycin solution (10,000 U/mL penicillin and 10 mg/ml streptomycin) were obtained from Lonza (Verviers, Belgium). The 75 cm^2 flasks, 96-well and 24-well plates were obtained from TPP (Trasadingen, Switzerland).

2.2 Methods

2.2.1 Ethyl acetate fraction (EAF)

The polyphenol-rich ethyl acetate fraction (EAF) from *Punica granatum* peel extract was obtained following the method described by [13] with some modifications. Briefly, the *P. granatum* fruit peel dry extract was commercially bought and then extracted for 24 hour by dynamic maceration with methanol containing 10% (v/v) of water. The obtained extract was dried *in vacuo* and then suspended in 2% aqueous acetic acid. The suspended extract was partitioned with dichloromethane and ethyl acetate. After that, the pooled ethyl acetate fractions were evaporated to dryness *in vacuo*.

2.2.2 Preparation of nanoemulsions

EAF-loaded pomegranate seed oil nanoemulsions (EAF-PSO-NE) were prepared using a ultrasonic emulsification method followed by solvent evaporation [14]. Briefly,

the ethyl acetate fraction (EAF) (0.5%; w/v), soy lecithin (0.4%; w/v) and PSO (2%; w/v) were dissolved in 10 mL of ethyl acetate. This ethyl acetate solution was slowly poured into 40 mL of a polysorbate 80 (2.1%; w/v) aqueous solution, and then it was adjusted to pH 5.0-6.5 with triethanolamine. The oil in water dispersion was sonicated for 3 minutes using an Ultrasonic Processor UP200S (Hielscher, Germany), and kept under magnetic stirring for 24 hours. The resulting nanoemulsion was evaporated under reduced pressure up to volume of 15 mL.

EAF-loaded medium chain trygliceride nanoemulsions (EAF-MCT-NE) were prepared by using the spontaneous emulsification method [15]. For that, 10 mL of an ethanolic solution containing EAF (0.5%; w/v), soy lecithin (0.4%; w/V), and MCT (1.8%, w/v) was poured into a 2.1% (w/v) polysorbate 80 aqueous solution and adjusted to pH 5.0-6.5 with triethanolamine, under magnetic stirring. The NE was then evaporated under reduce pressure to eliminate the organic solvent and concentrated up to volume of 15 mL. All formulations were filtered through 8 µm quantitative filter paper. Unloaded PSO-NE and MCT-NE were prepared in the same manner.

2.2.3 Droplet size and zeta potencial

Droplet size and zeta potencial were analyzed by dynamic light scattering (DLS) using a Malvern Zetasizer Nano ZS (Malvern Instruments Ltd, UK) at 25ºC and detection angle of 173º. Before measurement unloaded and EAF-loaded NE were appropriately diluted in ultrapurified water, or cell culture medium with 5% (v/v) FBS. Readings were taken immediately after preparation (t = 0 h) and after a 24 h incubation at 37 ºC (t = 24 h). Each measurement was performed using at least three sets of a minimum of 10 runs.

2.2.4 Culture of HaCat and 3T3 cell line

The spontaneously immortalized human keratinocyte cell line HaCat and the murine Swiss albino 3T3 fibroblast cell line were grown in DMEM medium (4.5 g L^{-1} glucose) supplemented with 10% fetal bovine serum, 2 mM L-glutamine, penicillin (100 U mL^{-1}) and streptomycin (100 µg mL^{-1}) at 37 ºC, 5% CO_2. Both cell lines were routinely cultured into 75 cm^2 culture flasks and trypsinized using trypsin/EDTA when the cells reached approximately 80% confluence.

2.2.5 Cytotoxicity assays

The cytotoxic effect of the free EAF, unloaded and EAF-loaded NE was measured by tetrazolium salt MTT assay [16] and neutral red uptake (NRU) assay [17]. 3T3 and HaCat cells were seeded into the central 60 wells of a 96-well plate at a density of 8.5 x 10^4 cells ml^{-1} and 1 x 10^5 cells ml^{-1}, respectively. After incubation for 24 h under 5% CO2 at 37 ºC, the spent medium was replaced with 100 µL of fresh medium supplemented with 5% FBS containing free EAF, unloaded or EAF-loaded NE at the required concentration range (7.8-500 µg mL^{-1}). After 24 h, the surfactant-containing medium was removed, and 100 µL of MTT in PBS (5 mg mL^{-1}) diluted 1:10 in medium without FBS and phenol red was then added to the cells. Similarly, 100 µL of 50 µg mL^{-1} NR solution in DMEM without FBS and phenol red was added in each well for the NRU assay. The plates were further incubated for 3 h, after which the medium was removed, and the cells were washed once in PBS. Thereafter, 100 µL of DMSO was added to each well to dissolve the purple formazan product (MTT assay) and for the NRU assay, 100 µL of a solution containing 50% ethanol absolute and 1% acetic acid in distilled water was added to extract the dye. After 10 min on a microtiter plate shaker at room temperature, the absorbance of the resulting solutions was measured at 550 nm using a Bio-Rad 550

microplate reader. The effect of each treatment was calculated as a percentage of cell viability inhibition against the respective controls.

2.2.6 Cryo-TEM

The morphology and size of the unloaded and EAF-loaded NE were analysed by cryo transmission electron microscopy (Cryo-TEM). Briefly, 5 µL of unloaded or EAF-loaded NE were appropriately diluted in ultrapure water or cell culture medium with 5% (v/v) FBS were placed on a Lacey carbon films on 200 mesh copper grids and automatically blotted against filter paper, leaving thin sample films spanning the grid holes. These films were vitrified by plunging the grids into ethane, which was kept at its melting point by liquid nitrogen, using a Vitrobot (FEI Company, Eindhoven, Netherlands) and keeping the sample before freezing at 100% humidity. The temperature at which the thin films and vitrification was initiated was room temperature. The vitreous sample films were transferred to a microscope Tecnai F20 (FEI Company, Eindhoven, Netherlands) using a Gatan cryo-transfer. The images were taken at 200 Kv with a 4096x4096 pixel CCD Eagle camera (FEI Company, Eindhoven, Netherlands) at a temperature between -170 ºC and -175 ºC and using low-dose imaging conditions.

2.2.7 Cell uptake studies

2.2.7.1 Intracellular localization of Nile red-labelled nanoemulsions

Nanoemulsion (NE) with nile red (NR) loaded (NR-NE) were prepared using PSO or MCT as oil phase. HaCat cells were plated in 24-well plates at a density of 1×10^5 cells/mL on round cover glasses (Marlenfeld GmbH & Co.KG, Lauda-Könlgshofen, Germany) and incubated overnight at 37 ºC under 5% CO_2. When cells reached

confluence, the culture medium was replaced with fresh medium containing NR-NE at a final concentration of 25 μg mL^{-1} and incubated for 2 and 24 h. After incubation, the samples were aspirated and the cells were washed four times with PBS and fixed with 4 % (v/v) formaldehyde in PBS (pH 7.4) for 15 min at room temperature and away from light. The individual cover glasses were then mounted on clean glass slides with a drop of Prolong® Gold antifade reagent (Invitrogen, OR, USA) for subsequent fluorescence microscopy analysis (Olympus BX41 microscope equipped with a UV-mercury lamp, 100 W Ushio Olympus, and a filter set type MNIGA3 540-550 nm excitation, 575-625 nm emission and 570 nm dichromatic mirror). Images were digitized on a computer through a video camera (Olympus digital camera XC50) using an image processor (Olympus cell^B Image Acquisition Software). To calculate the mean fluorescence value of the cells, approximately 40 individual cells from different fields and images were analyzed with ImageJ software (version 1.46, National Institutes of Health, MD, USA) and their total fluorescence intensity was quantified, which corresponds to the cell internalization of nanoemulsion [18].

2.2.7.2 Intracellular release of calcein

HaCat cells were plated (1×10^5 cells/mL) in 24-well plates on round cover glasses (Marlenfeld GmbH & Co.KG, Lauda-Könlgshofen, Germany) and incubated at 37 ºC under 5% CO_2 until confluence was reached. Then calcein, a membrane-impermeable fluorophore, at 1 mg mL^{-1} was added to the cells as a tracer molecule to monitor the effect of the EAF-loaded NE on endosomes after cell internalization (control). EAF-loaded NE in the concentration of 50 μg mL^{-1} with calcein, were diluted in DMEM medium without FBS and phenol red. After 2 h incubation at 37 ºC, the cells were washed four times with PBS and incubated in DMEM medium with 10% FBS for 3 h to allow intracellular

trafficking. Then cells were washed four times with PBS and fixed with 4% (v/v) formaldehyde in PBS (pH 7.4) for 15 min at room temperature. Individual cover glasses was mounted on a clean glass slide with Prolong® Gold antifade reagent (Invitrogen, OR, USA) and analysed on a Olympus BX41 fluorescence microscope equipped with a UV-mercury lamp (100 W Ushio Olympus) and a filter set type MNIBA3 (470-495 nm excitation, 510-550 nm emission and 505 nm dichromatic mirror). Images were digitized on a computer through a video camera (Olympus digital camera XC50) using an image processor (Olympus cell^B Image Acquisition software).

ImageJ software was used to calculate the average pixel intensity of calcein fluorescence within regions of interest (ROI) drawn on to collected images. This was done by drawing three ROI inside the cell (excluding any calcein-containing vesicles and, thus, representing the cytoplasm only) and the results were obtained in arbitrary fluorescence units. Images of ~40 individual cells were analysed for each formulation. [18].

2.2.8 UVB photoprotection *in vitro* studies

Treatment of keratinocytes with EAF and nanoemulsions

(A) To evaluate the photoprotective effect of free EAF and EAF-loaded NE, HaCat cells were pre-treated (1 hour; cell incubator) with 20 µg mL^{-1} or 50 µg mL^{-1} of each sample in serum-free medium without phenol red, irradiated and incubated at 37 ºC for another 2 hours.

(B) To verify the photorepair activity, HaCat cells were first irradiated (90 mJ/cm^2), then treated with free EAF, unloaded or EAF-loaded NE (50 µg mL^{-1}) in serum-free medium and incubated at 37 ºC for 24 hours.

UVB irradiation

The keratinocytes were UVB irradiated (90 or 200 mJ/cm^2) in culture plates

placed under a Philips LP471 UVB source, with a spectral range of 280-315 nm. In parallel, non-irradiated cells were treated similarly and kept in the dark in a cell incubator. The UVB output measured by an UVB-meter (Delta OHM HD 2302.0) before each experiment in direct contact with the cell culture plate was 0.4 mW/cm^2.

2.2.9 Comet assay (single cell gel electrophoresis assay – SCGE)

Two (photoprotection) or 24 hours (photorepair) after irradiation, the cells from two wells of each treatment were trypsinised, transferred to eppendorfs and centrifuged at 1500 rpm for 5 minutes. Microscope slides containing the samples (cells pellet) mixed with 0.9% solution of low-melting point agarose were prepared. The cells were lysated and then incubated in alkaline electrophoresis buffer for DNA unwinding and conversion of alkali-labile sites to single-strand breaks. Electrophoresis was performed in the same buffer for 30 min at 25 V and 300 mA. After that, 30 µL of 5 µg/mL DAPI solution was added to each slide for the fluorescence microscopy analysis. The migration of nuclear DNA from the cells was measured using the COMET ASSAY IV® Program (Perspective Instruments) for 50 randomly selected cell images and the mean percentage of DNA in the tail (% Tail DNA) was calculated in each trial.

2.2.10 Interleukin-8 determination

The effect of UVB and treatments on IL-8 was determined using a specific immunoassay kit BD OptEIA™ Set for human interleukin-8 (BD Biosciences, USA) according to the manufacturer's protocol. Briefly, after centrifugation time (see *Comet assay item 2.9.3*), the supernatant was collected and samples were stored at -20ºC. One hundred microliters of samples were transferred to a 96-well plate, covered with a specific capture antibody and incubated (2 h at room temperature). The mixture was removed,

wells were rinsed five times with wash buffer and the detection antibody solution was added (1 h at room temperature). Then the solution was removed, the wells were rinsed seven times with wash buffer and the substrate solution was added. After incubation (30 min at room temperature, in the dark), stop solution was applied and a yellow-colored product was measured at 450 nm using a Bio-Rad 550 microplate reader.

2.2.11 Sun protector factor determination *in vitro*

The *in vitro* sun protection factor (SPF) of the free EAF, EAF-loaded NE and PSO were determined according to the method previously described [19]. Dilute solutions of free EAF and EAF-loaded NE were tested at concentrations of 5, 20, 50 and 100 µg mL^{-1}; PSO was tested at 20, 80, 200 and 400 µg which correspond to the amount of oil found in each concentration mentioned of NE. The absorption spectra of samples were obtained in the range of 290 to 320 nm every 5 nm, using 1 cm quartz cell. The observed absorbance values were calculated by using the equation:

$$SPF_{spectrophotometric} = CF \times \sum_{290}^{320} EE(\lambda) \times I(\lambda) \times Abs(\lambda)$$

Where: CF – correction factor (10), EE (λ) – erythemal effect spectrum, I (λ) – solar intensity spectrum, Abs (λ) – absorbance values at wavelength λ. The values of EE × I are constants and were determined by [20].

2.2.12 Phototoxicity test

The phototoxicity test was carried out as described in the Organization for Economic Co-operation and Development (OECD) 432 guidelines with some modification. Cell lines 3T3 and HaCat were used as *in vitro* models to predict the

cutaneous phototoxicity. Briefly, 3T3 mouse fibroblast cell line and HaCat cell line were maintained in culture for 24 h for formation of monolayers. Two 96-well plates per cell line were then pre-incubated in six duplicate with EAF, EAF-PSO-NE and EAF-MCT-NE at 50 µg mL^{-1} for 1h. One plate of each cell line was then exposed to a dose of 5 J/cm^2 UVA (+Irr experiment), whereas the other plate was kept in the dark (-Irr experiment). UVA irradiation was performed using a TL-D 15 W/10 UVA lamp (Royal Philips Eletronics-The Netherlands), with a spectral range of 315-400 nm. The treatment medium was then replaced with culture medium and, after 24 h, cell viability was determined by neutral red uptake assay. The neutral red uptake was measured after 3 h incubation at the absorbance of 550 nm using a Bio-Rad 550 microplate reader. Cell viability obtained with each sample at 50 µg mL^{-1} in both cell lines was compared with that of untreated controls and the percent inhibition was calculated. To predict the phototoxic potential, the cell viabilities obtained in the presence and in the absence of UVA radiation were compared. The photoirritation factor (PIF) was determined as follows:

$$PIF = \frac{Cell\ viability\ (-Irr)}{Cell\ viability\ (+Irr)}$$

2.2.13 Statistical analysis

Each experiment was run at least on triplicate. Statistical analysis were performed using one-way analysis of variance (ANOVA) followed by Dunnett's or Tukey's post-hoc test for multiple comparisons using Instat software. Differences were considered significant for $p < 0.05$.

3. Results and Discussion

3.1 Characterization of nanoemulsions

The EAF and EAF-loaded NE were developed and characterized according to physico-chemical properties. The EAF presented a substantial amount of total phenolic compounds (around 638 mg g^{-1} GAE – gallic acid equivalents), being ellagic acid, gallic acid and punicalagin the major ones. The entrapment efficiency of the phenolic compounds in the nanoemulsions was near or above 50% depending on the chemical compound lipophilicity. Furthermore, the antioxidant activity through DPPH and FRAP assay was determined (Article accepted).

A characterization of the nanodispersion when in contact with the cell culture medium, is extremely important since the nanosystem and its components do not always behave as inert objects. The cell growth media contains serum proteins, essential amino acids, vitamins, electrolytes, and other chemicals. These various components could interact with nanoparticles/nanodroplets and change their physicochemical properties and stability [21]. Rather nanoparticles/nanodroplets can undergo aggregation or agglomeration, proteins present in biological medium can adsorb and change the features of the nanosystem interaction with cells [22-24]. The unloaded and EAF-loaded NE were characterized in size, zeta potential and PI when dispersed in cell culture medium (DMEM 5% FBS).

Table 1 shows the DLS measurements of unloaded and EAF-loaded NE right after being diluted in ultrapure water or in culture medium DMEM 5% FBS at time 0 and 24h of incubation. The size of unloaded PSO-NE and MCT-NE did not alter when incubated in cell culture medium; EAF-PSO-NE and EAF-MCT-NE showed an increase of about 20% in particle size mainly after 24 h incubation in cell culture medium, increasing from

203 nm to 244 nm and from 185 nm to 218 nm, respectively. The zeta potential values of unloaded and EAF-loaded NE when diluted in ultrapure water were high negative, similar to the value previously reported (Article accepted), whereas almost close to zero values were obtained in cell culture medium. The first hypothesis for size augmentation and surface charge decreasing is that in the presence of non-ionic surfactants (i.e. polysorbate) the protein adsorption layer could be formed by hydrophobic interaction with the surfactant. The second hypothesis is that for water/oil interface the adsorbing protein molecules could penetrate into the hydrophobic oil phase with the hydrophobic parts of the molecule [25]. As observed from the PI values of the unloaded and EAF-loaded NE, after the incubation in cell culture medium the nanometric-sized dispersion remained as monodisperse (PI<0.3). Cryo-TEM images (Figure 1) corroborated the mean hydrodynamic size obtained by DLS. Some limited particle deformation can be seen in the cryo-TEM image due to the confining effect inside the thin film of vitreous ice [26].

Table1. Characterization of *P. granatum* unloaded and EAF-loaded nanoemulsions in water and culture medium DMEM 5% FBS at incubation time 0 and 24 h.

Nanoemulsions	***Ultrapure Water***			***5% FBS - t0***			***5% FBS - t24 h***		
	Size (nm)	*Zeta Potential (mV)*	*PI*	*Size (nm)*	*Zeta Potential (mV)*	*PI*	*Size (nm)*	*Zeta Potential (mV)*	*PI*
EAF-PSO-NE	203.2 ± 1.8	-28.9	0.222	211.4 ± 4.0	-4.8	0.217	244.4 ± 0.9	-5.6	0.251
PSO-NE	146.1 ± 0.6	-18.6	0.124	150.2 ± 1.2	-3.6	0.121	151.2 ± 1.1	-3.0	0.123
EAF-MCT-NE	185.6 ± 0.8	-28.3	0.154	193.2 ± 1.4	-4.4	0.191	218.3 ± 1.3	-4.4	0.221
MCT-NE	168.7 ± 0.1	-15.3	0.174	170.3 ± 0.8	-1.5	0.167	170.5 ± 0.8	-3.3	0.197

PI = Polidispersity Index; Values are expressed as mean ± SD (n=3).

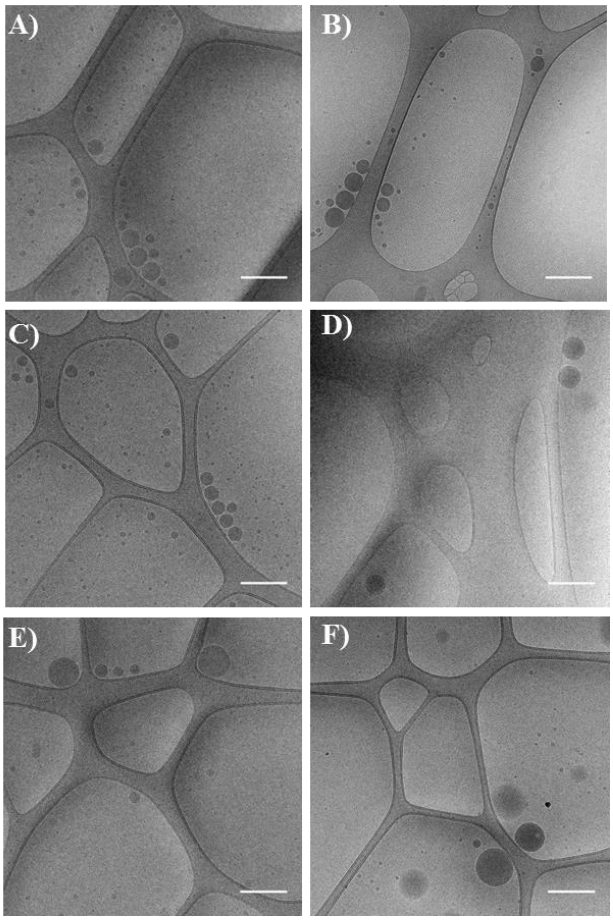

Figure 1. Cryo TEM image of *P. granatum* unloaded and EAF-loaded nanoemulsions. Formulations dispersed in ultrapurified water: (A) MCT-NE; (B) EAF-MCT-NE; (C) PSO-NE; (D) EAF-PSO-NE; Formulations in DMEM 5% FBS after 24 h incubation: (E) EAF-MCT-NE and (F) EAF-PSO-NE. Scale bars corresponds to 500 nm.

3.2 Cell viability studies

In vitro cell-culture based cytotoxicity is a highly used alternative to animal testing. To determine the IC_{50} of free EAF, unloaded and EAF-loaded NE two endpoints assays were used - one concerning the mitochondrial compartment integrity (MTT) and other the lysosomal damage (NRU). The cytotoxicity of free EAF, unloaded and EAF-loaded NE was assessed in human keratinocytes HaCat and fibroblast 3T3 cell lines (Table 2). In general for the 3T3 cell line and both endpoint assays, the unloaded PSO-

NE and MCT-NE were more cytotoxic to the cells presenting a lower IC_{50} value, followed by free EAF and EAF-MCT-NE; the EAF-PSO-NE was the less cytotoxic with higher IC_{50}. For HaCat cell line the behavior was the other way around, the free EAF and unloaded NE were less cytotoxic than the EAF-loaded NE with a higher IC_{50} value in both endpoint assays. Indeed, the cytotoxic effects of free EAF, unloaded and EAF-loaded NE showed some disparities that, in fact, might depended on the NE components, cell line and endpoint assayed.

Moreover it is noteworthy that concentrations used in the experiments were much lower than the cytotoxic ones. Finally, in studies of MTT and neutral red dyes interactions with NE alone (without the cells) through UV-visible measurements, there was no interference of the formulations with the assays dyes (data not shown).

Table 2. Values of IC_{50} for free EAF, unloaded and EAF-loaded nanoemulsions in 3T3 fibroblast and HaCat keratinocytes.

Treatment	***MTT***		***NRU***	
Assay/cell line	***IC_{50} (μg mL^{-1})***		***IC_{50} (μg mL^{-1})***	
	3T3	*HaCat*	*3T3*	*HaCat*
EAF	116.5 ± 0.2	166.5 ± 5.7	105.7 ± 10.4	175.2 ± 11.1
EAF-PSO-NE	168.9 ± 8.3	79.0 ± 15.2	89.0 ± 6.4	94.1 ± 1.2
EAF-MCT-NE	115.5 ± 13.6	93.2 ± 1.2	71.3 ± 9.8	93.4 ± 0.8
PSO-NE	89.5 ± 0.3	107.1 ± 6.9	91.5 ± 11.7	190.3 ± 3.7
MCT-NE	74.7 ± 11.7	132.9 ± 12.7	79.9 ± 4.2	164.0 ± 1.8

Values are expressed as mean ± SD of at least three independent experiments.

3.3 Cellular internalization studies

The cell uptake of fluorescent-labelled NR-NE nanodroplets by the HaCat cell line was visualized by a fluorescence microscope after 2 and 24 h incubation (Figure 2A). It was observed that the nanodroplets were taken up by the cells since some fluorescent punctate spots were seen in the cell cytosol. However, a bigger number of fluorescent spots were detected along the cell membrane. After 24 h incubation a more intensive dotted pattern of fluorescent NR-NE nanodroplets was observed inside the cell, but again, predominantly along the cell membrane together with some diffuse fluorescence. Figure 2B shows the quantitative analysis of the images and it corroborates to the fact that after 24 h incubation there is an increase of NR-NE nanodroplets inside the cell but a much greater and intense localization is seen along the cell membrane.

It was reported that neutral and negatively charged particles adsorbed much less on the negatively charged cell-membrane surface and consequently show lower levels of internalization as compared to the positively charged particles [27-29]. These finding is in agreement with our results obtained for cell internalization of EAF-loaded NE studies. In general, a certain amount of nanodroplets were internalized by the cells, probably through nonspecific binding of the nanodroplets on relatively scarcer cationic sites on the plasma membrane and their subsequent endocytosis [27], due to the fact that the nanoemulsions contain anionic surfactant and present a great amount of hydroxyl groups from the polyphenolic compounds in the EAF.

Figure 2C shows the ability of EAF-loaded NE to destabilize the endosomal membrane and release the endocytosed material into the HaCat cell cytoplasm. The uptake of calcein, a membrane-impermeable fluorophore, and EAF-loaded NE into keratinocyte HaCat cells was observed through fluorescence microscopy. The control cells, treated with calcein alone, presented a punctate distribution, which is consistent

with constitutive endocytosis of the external medium and indicates that the endosome membranes were not damaged [18, 30]. When the calcein was co-incubated with EAF-loaded NE a diffuse fluorescence into the cell cytoplasm was observed in some cells which suggest a low release of calcein from endosomal compartments. However, the quantitative analyses of the cytosolic calcein distribution (Figure 2D) shows that this fluorescence observed was not great enough to be statistically different from the control cells.

Since the main phenolic compounds identified and quantified in the EAF (ellagic acid, gallic acid and punicalagin) are partially in the ionized form (hydroxyl anion) at pH range of endosomal compartments (pka=5.5; 5.0 and 5.12, respectively) an interaction between the EAF-loaded NE and the endosomal membrane and consequently release of endocytosed material into the cytoplasm might be difficult. However, EAF-loaded NE may act in the extracellular medium and through cell membrane lipid bilayer (inner and outer layer) without compromising its integrity, as demonstrated in our previous study (Article submmited). Obviously, the possibility of the EAF-loaded NE reaching the cytosol compartment through another internalization pathway cannot be discarded.

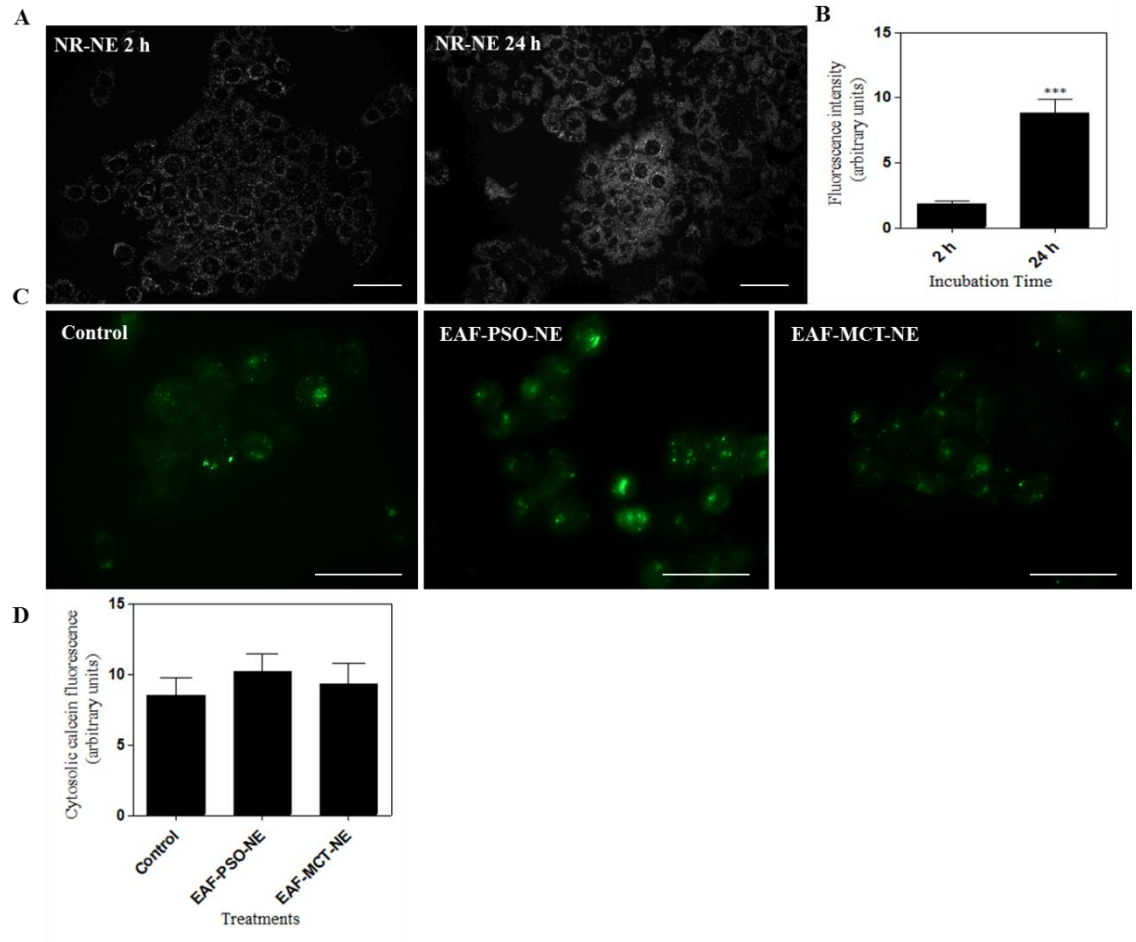

Figure 2. (A) Localisation of NR-NE by HaCat cells after 2 and 24 h of incubation at 37 ºC. Cell uptake was visualized using fluorescence microscopy. (B) Quantitative fluorescence analysis of images like those in 'A'. (C) Fluorescence microscopy images of HaCat cells showing the distribution of calcein fluorescence. The cells were treated with 1 mg mL^{-1} of calcein (control) and both 1 mg mL^{-1} of calcein and 50 µg mL^{-1} of each EAF-loaded NE formulation. Images were acquired at 3 h after 2 h of uptake. (D) Quantitative fluorescence analysis of images like those in 'C'. Scale bar: 50 µm. The results represent the mean value of ~ 40 cells ± SEM. Statistical analyses were performed using ANOVA test ($^{***}p < 0.001$).

3.4 Photoprotection against UVB-induced DNA damage

EAF-loaded NE and free EAF were capable to protect the human keratinocyte HaCat cells from UVB-induced DNA damage, as shown in Figure 3. When cells were irradiated at a dose of 90 mJ/cm^2 both the EAF-loaded NE and free EAF concentrations tested , 20 and 50 μg mL^{-1}, were able to protect and reduce cell DNA damage in a dose dependent manner. At dose of 200 mJ/cm^2, only the concentration of 50 μg mL^{-1} was effective. There was no statistically difference between free EAF and EAF-loaded NE on the photoprotection against UVB-induced DNA damage, which means that even when entrapped into the oil phase the EAF is able to deliver the same protection. The unloaded NE did not protect the cells against UVB-induced DNA damage (data not shown).

The EAF-loaded NE and free EAF could not repair the DNA damage after UVB radiation (data not shown), only protect. However, when MTT assay was employed to characterize keratinocytes cells viability after UVB radiation at dose of 90 mJ/cm^2 (Figure 4), the cells that were irradiated and then treated with free EAF or EAF-loaded NE, were statistically more viable after 24 h than the untreated control or the unloaded NE treated cells, this latter presented cell viability as the untreated control cells (data not shown).

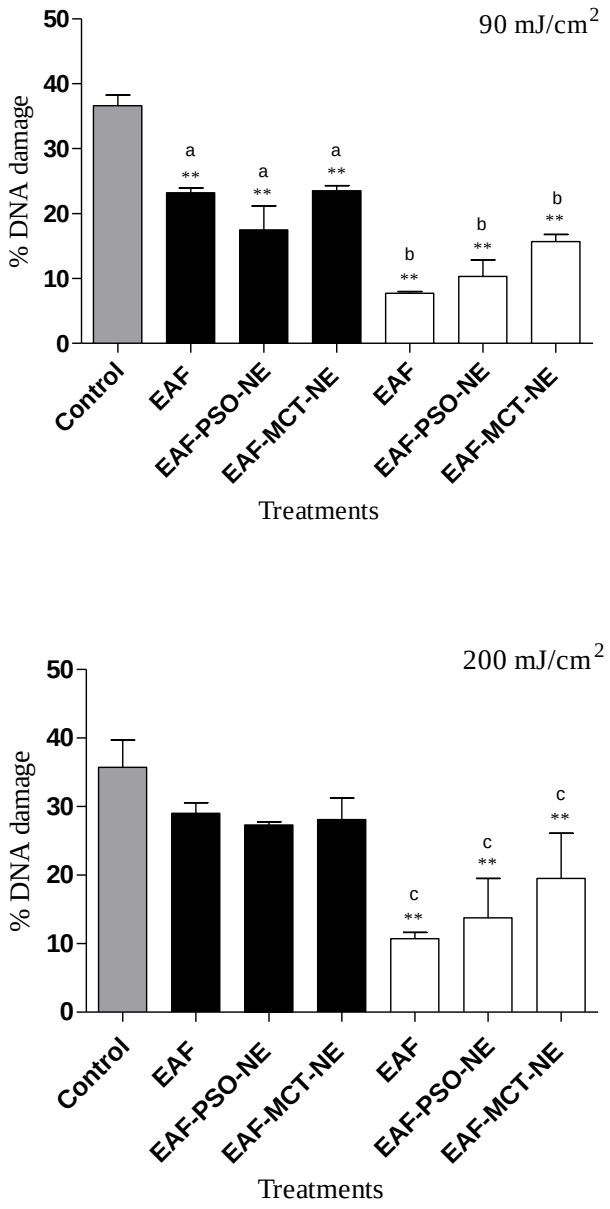

Figure 3. Photoprotection of *P. granatum* free EAF and EAF-loaded nanoemulsions (EAF-PSO-NE and EAF-MCT-NE) against UVB-induced DNA damage at irradiation dose of 90 mJ/cm^2 and 200 mJ/cm^2. Black bars means concentration of 20 µg mL^{-1} and white bars 50 µg mL^{-1}. ** $p < 0.01$ when compared to non-treated irradiated control. Data is presented as mean ± SEM. Same letters means no statistical difference – ANOVA followed by Tukey's post-hoc test for multiple comparisons.

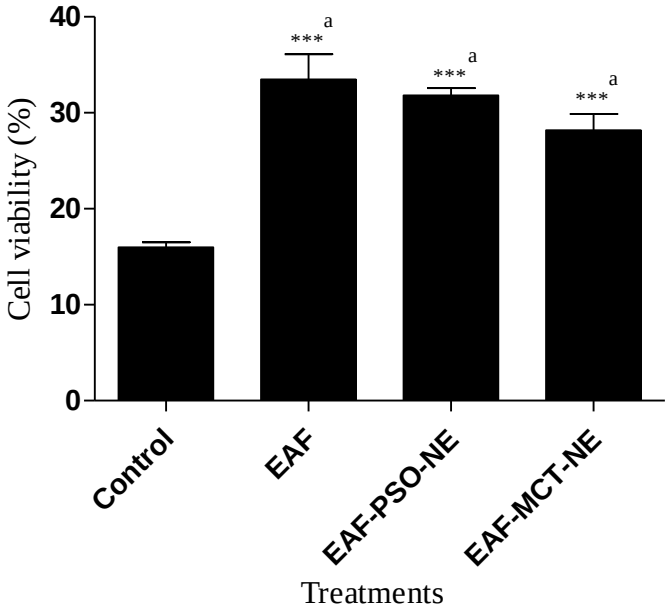

Figure 4. Keratinocytes HaCat cell viability measured by MTT assay after UVB irradiation and 24 h incubation at photorepair conditions (*see methods section for more details*). Cells were treated with *P. granatum* free EAF and EAF-loaded nanoemulsions. *** $p < 0.001$ when compared to non-treated irradiated control. Data is presented as mean ± SEM. Same letters means no statistical difference – ANOVA followed by Tukey's post-hoc test for multiple comparisons.

The use of botanical compounds as photoprotective agents in dermatological preparations gained a considerable attention since these chemical compounds exhibit a wide range of biological activities [31] and act either as filters, absorbing the UVB photons, or by the antioxidant activity mainly of the polyphenolic constituents preventing from photooxidative damage. Previously, high concentrations of total phenolics and substantial amounts of ellagic acid, gallic acid and punicalagin were quantified in the free EAF and EAF-loaded NE through a HPLC-DAD method (Article accepted). Here, we evaluated the pre-treatment and post-treatment (photorepair) with free EAF, unloaded and EAF-loaded NE on UVB-induced DNA damage in keratinocytes.

DNA bases are considered to be the main targets (chromophores) of UVB irradiation, which result in base modification or dimmer formation [2]. The DNA lesions observed in the comet assay after UVB irradiation are thought to be transient DNA breaks during the nucleotide excision repair of the photoprodutcs [32, 33]. Other mecanisms including oxidative damage to DNA due to the excess of reactive oxygen species (ROS) generation may also contribute to the UVB-induced comet formation [1, 3, 31]. At the concentration of 50 μg mL^{-1} free EAF and EAF-loaded NE application protected the cells from UVB-induced DNA damage up to a dose of 200 mJ/cm^2. Treatments did not promote DNA repair after 24 h incubation but were able to enhance the cell viability in approximately 50%. Our result corroborates the reports from other authors on the photoprotection activity of pomegranate fruit extract and derived products [34-37].

3.5 Interleukin-8 release

Figure 5 shows the IL-8 release by keratinocytes cells after UVB irradiation doses of 90 mJ/cm^2 and 200 mJ/cm^2 or at photorepair conditions. Similarly to the photoprotection results, the free EAF and EAF-loaded NE at 50 μg mL^{-1} reduced the IL-8 release in irradiated cells when they were applied before UVB exposure and after (photorepair). The maximal protection reached was around 80% for the free EAF and EAF-loaded NE and these treatments were statistically the same. The cells treated with the unloaded NE released a great amount of IL-8 as the untreated control cells (data not shown).

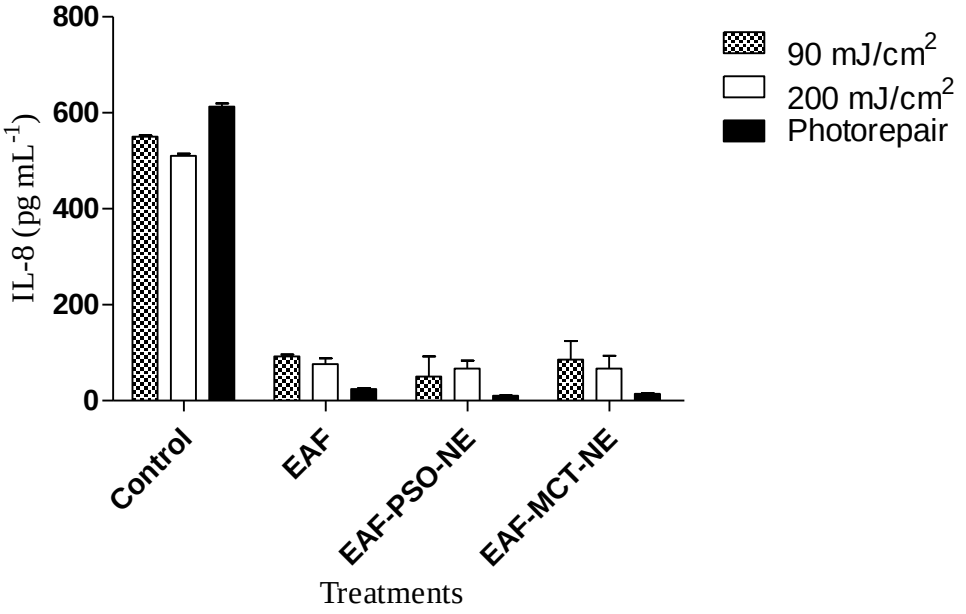

Figure 5. UVB induced IL-8 in keratinocytes HaCat after irradiation doses of 90 mJ/cm^2 and 200 mJ/cm^2 or at photorepair conditions (*see methods section for more details*). Cells were treated with *P. granatum* free EAF and EAF-loaded nanoemulsions at 50 µg mL^{-1}. Data is presented as mean ± SEM.

Reduction of UVB-induced IL-8 secretion by keratinocytes demonstrates an important mechanism for protection against UVB-induced skin inflammation by free EAF and EAF-loaded NE, since these cytokine is upregulated in human keratinocytes following UVB-irradiation *in vitro* and *in vivo* [38, 39]. Significant IL-8 concentrations were secreted and released by the cells in the medium after the UVB radiation, and the EAF and EAF-loaded NE were able to suppress the secretion up to basal IL-8 concentrations. IL-8, a pro-inflamatory and chemotactic cytokine is a key mediator of UVB-induced inflammation, acting as a potent chemoattractant for neutrophils, which then cause local tissue damage [40]. Furthermore, IL-8 induces keratinocyte proliferation, angiogenesis and growth of a variety of tumors and enhances expression of matrix metalloproteinases (MMPs) [41, 42].

3.6 Sun protector factor determination

The SPF *in vitro* was determined for free EAF, EAF-loaded NE and PSO by the spectrophotometric method using the UVB region. In Figure 6, it can be observed that the EAF-PSO-NE showed the higher SPF at almost all concentrations tested (20, 50 and 100 μg mL^{-1}) except for the 5 μg mL^{-1}, when EAF-PSO-NE, free EAF and PSO presented statistically the same SPF (~2). The highest SPF value (~25) was verified for EAF-PSO-NE at 100 μg mL^{-1}. Also the SPF values obtained for all samples were concentration-dependent. The sun protection factor (SPF) is the universal indicator for describing the efficiency of sunscreen products. The *in vitro* method correlates well with the *in vivo* tests because it relates the absorbance of the substance with the erythematogenic effect of radiation and intensity of light at specific wavelenghs between 290 and 320 nm [43-48]. A synergic effect was visualized between the PSO and the EAF. Besides the phenolic compounds verified in the EAF, PSO presents a typical fatty acid profile which includes high concentration of the punicic acid (~65%), a polyunsaturated acid with three conjugated double bonds in the molecule that also absorbs light.

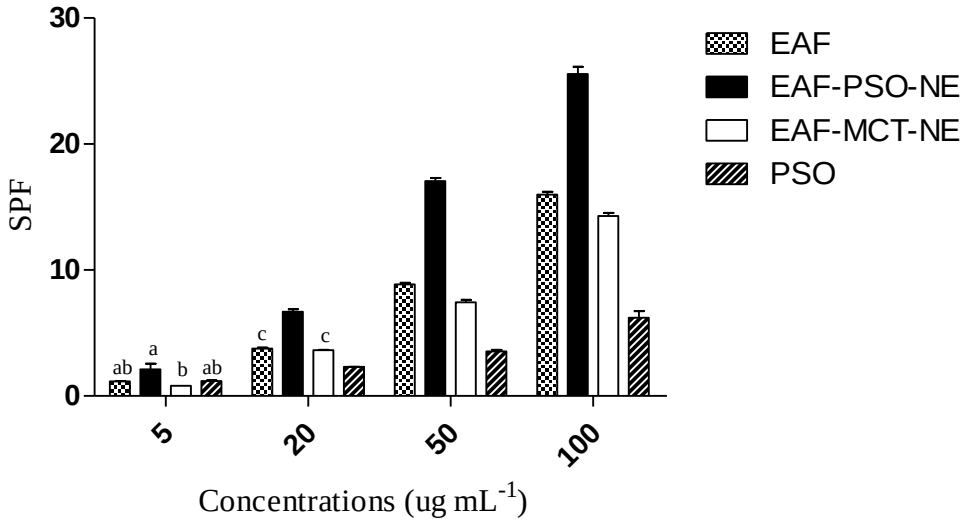

Figure 6. Spectrophotometrically calculated sun protector factor (SPF) values of *P. granatum* ethyl acetate fraction fraction (EAF), seed oil (PSO) and EAF-loaded nanoemulsions (EAF-PSO-NE and EAF-MCT-NE). Data is presented as mean ± SD. Same letters means no statistical difference – ANOVA followed by Tukey's post-hoc test for multiple comparisons.

3.7 Phototoxicity

In vitro 3T3 NRU phototoxicity test is a highly sensitive alternative methodology for evaluating phototoxic risk for both pharmaceutic and cosmetic formulations, especially photoirritant risk. Photoirritation is an inflammatory event in the skin that sometimes is induced by oxidative stress in the cellular membrane, triggered by both excessive accumulation of photosensitizers in the skin and exposure of the skin to a particular wavelength of light [49]; photo-oxidation of lipids and proteins and binding of photosensitizers to amino acid moieties in cellular membrane are two commonly causative reactions on photoirritation [50, 51]. The phototoxicity of free EAF and EAF-loaded NE were evaluated on 3T3 mouse fibroblast and HaCat human keratinocytes measured by NRU assay. The cell viability (%) was mostly above 80% for non-irradiated

and irradiated cells line. The photoirritant factor (PIF), which was calculated by dividing the cell viability of non-irradiated cells plate by the cell viability of UVA irradiated cells plate of each treatment at a concentration of 50 µg mL^{-1}, was found to be 1<PIF<2 that classifies the treatments at the concentration tested as non-phototoxic [52]. These results corroborated the preliminary photosafety evaluation of EAF-loaded NE and free EAF in human red blood cells model demonstrated in our previous study (article submmited).

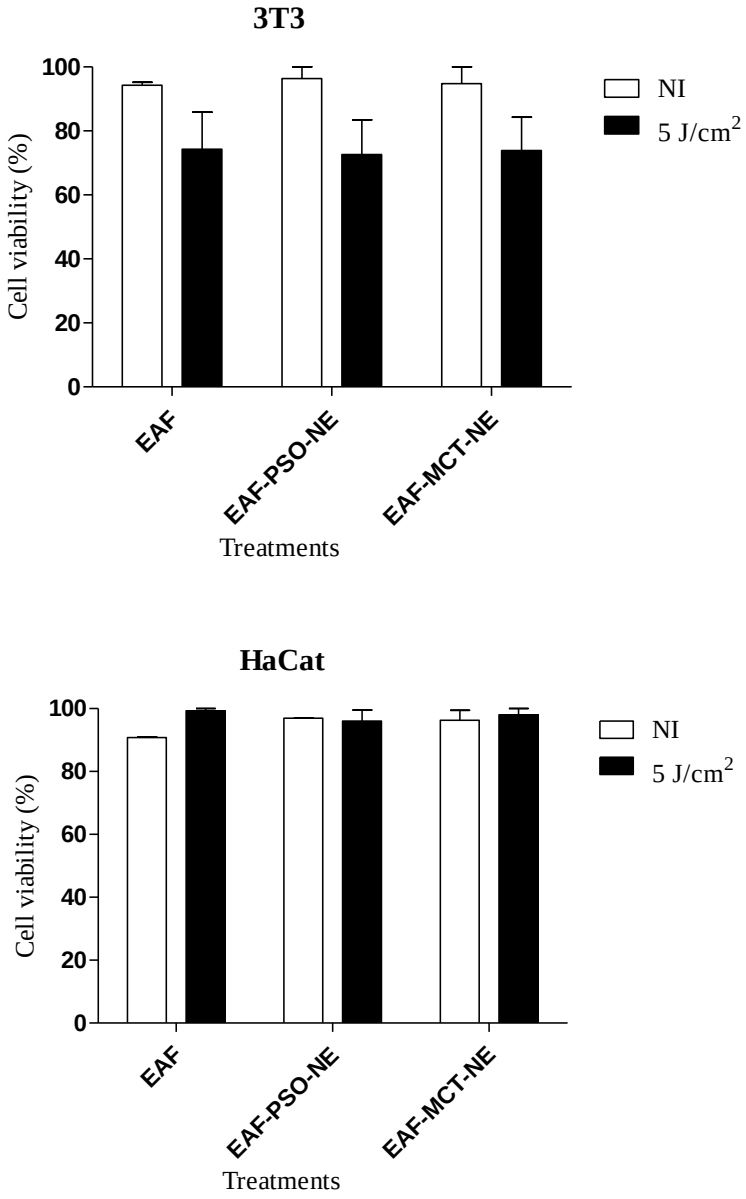

Figure 7. Phototoxicity of free EAF and EAF-loaded nanoemulsions (EAF-PSO-NE and EAF-MCT-NE) at 50 µg mL^{-1} on 3T3 mouse fibroblast and HaCat human keratinocytes measured by NRU assay. White bars means non-irradiated cells and black bars UVA 5 J/cm^2 irradiated cells. Data is presented as mean ± SEM.

4. Conclusions

Our results suggests that pomegranate seed oil nanoemulsion entrapping pomegranate peel polyphenol-rich extract has a great potential to be used as a sunscreen. EAF-loaded NE were able to internalized the keratinocyte cell and also accumulate along the cell membrane. Formulations protected the cell DNA against UVB-induced damage, and it was concentration dependent. The SPF determined for EAF-loaded NE was considerably high taking into account no synthetic filters were involved. No phototoxic effect was observed after incubation of EAF or EAF-loaded NE with 3T3 mouse fibroblasts or human keratinocytes HaCat. All the data presented here can be considered a starting point for the initiation of the use of pomegranate seed oil nanoemulsion entrapping pomegranate peel polyphenol-rich extract for the photoprotection against UVB radiation and its damaging effects on the human skin. However, further studies are needed to be conducted for better understanding of this photoprotective effect.

Conflict of Interest

The authors report no conflicts of interest. The authors alone are responsible for the content and writing of the paper.

Acknowledgment

The authors acknowledge the financial support from CAPES for the financial support (CAPES/PDSE Project No. BEX 5613/13-2), Ministerio de Economía y Competitividad - Spain (Project MAT2012-38047-C02-01) and FEDER (European Union). The authors would like to thank Carmem Iglesias for her expert technical assistance on Cryo-TEM.

References

[1] J. Nichols, S. Katiyar, Skin photoprotection by natural polyphenols: anti-inflammatory, antioxidant and DNA repair mechanisms, Arch Dermatol Res, 302 (2010) 71-83.
[2] A. Svobodová, A. Zdařilová, J. Vostálová, Lonicera caerulea and Vaccinium myrtillus fruit polyphenols protect HaCaT keratinocytes against UVB-induced phototoxic stress and DNA damage, J. Dermatol. Sci., 56 (2009) 196-204.
[3] J. Vostálová, A. Zdařilová, A. Svobodová, Prunella vulgaris extract and rosmarinic acid prevent UVB-induced DNA damage and oxidative stress in HaCaT keratinocytes, Arch Dermatol Res, 302 (2010) 171-181.
[4] M. Perde-Schrepler, G. Chereches, I. Brie, C. Tatomir, I.D. Postescu, L. Soran, A. Filip, Grape seed extract as photochemopreventive agent against UVB-induced skin cancer, J. Photochem. Photobiol., B, 118 (2013) 16-21.
[5] M. Viuda-Martos, J. Fernández-López, J.A. Pérez-Álvarez, Pomegranate and its Many Functional Components as Related to Human Health: A Review, Compr Rev Food Sci Food Saf, 9 (2010) 635-654.
[6] J. Jurenka, Therapeutic applications of pomegranate (Punica granatum L.): a review, Alternative Medicine Review, 13 (2008) 128-144.
[7] I.L.P. Melo, E.B.T. Carvalho, J. Mancini-Filho, Pomegranate seed oil (Punica granatum L.): A source of punicic acid (conjugated alpha-linolenic-acid), Plant Foods Hum Nutr, 2 (2014) 1024.
[8] T. Ismail, P. Sestili, S. Akhtar, Pomegranate peel and fruit extracts: A review of potential anti-inflammatory and anti-infective effects, J Ethnopharmacol, 143 (2012) 397-405.
[9] S.Y. Schubert, E.P. Lansky, I. Neeman, Antioxidant and eicosanoid enzyme inhibition properties of pomegranate seed oil and fermented juice flavonoids, J Ethnopharmacol, 66 (1999) 11-17.
[10] S.A. Chime, F.C. Kenechukwu, A.A. Attama, Nanoemulsions — Advances in Formulation, Characterization and Applications in Drug Delivery, Intech Books, Croatia, 2014.
[11] T.G. Mason, J.N. Wilking, K. Meleson, C.B. Chang, S.M. Graves, Nanoemulsions: formation, structure, and physical properties, J Phys Condens Matter, 18 (2006) R635.
[12] A.P.C. Silva, B.R. Nunes, M.C. de Oliveira, L.S. Koester, P. Mayorga, V.L. Bassani, H.F. Teixeira, Development of topical nanoemulsions containing the isoflavone genistein, Pharmazie, 64 (2009) 32-35.
[13] P. Panichayupakaranant, A. Itsuriya, A. Sirikatitham, Preparation method and stability of ellagic acid-rich pomegranate fruit peel extract, Pharm Biol, 48 (2010) 201-205.
[14] C.P. Tan, M. Nakajima, β-Carotene nanodispersions: preparation, characterization and stability evaluation, Food Chem., 92 (2005) 661-671.
[15] K. Bouchemal, S. Briançon, E. Perrier, H. Fessi, Nano-emulsion formulation using spontaneous emulsification:solvent, oil and surfactant optimisation, Int J Pharm, 280 (2004) 241-251.
[16] T. Mosmann, Rapid colorimetric assay to cellular growth and survival:application to proliferation and cytotoxicity assays, J. Immunol. Methods, 65 (1983) 55-63.

[17] E. Borenfreund, J. Puerner, Toxicity determined in vitro by morphological alterations and neutral red absorptio, Toxicol. Lett., 24 (1985) 119-124.
[18] D.R. Nogueira, M.d. Carmen Morán, M. Mitjans, L. Pérez, D. Ramos, J.d. Lapuente, M. Pilar Vinardell, Lysine-based surfactants in nanovesicle formulations: the role of cationic charge position and hydrophobicity in in vitro cytotoxicity and intracellular delivery, Nanotoxicology, 8 (2014) 404-421.
[19] J.d.S. Mansur, M.N.R. Breder, M.C.d.A. Mansur, R.D. Azulay, Correlaçäo entre a determinaçäo do fator de proteçäo solar em seres humanos e por espectrofotometria, An. bras. dermatol, 61 (1986) 167-172.
[20] R.M. Sayre, P.P. Agin, G.J. LeVee, E. Marlowe, A comparison of in vivo and in vitro testing of sunscreening formulas, Photochem. Photobiol., 29 (1979) 559-566.
[21] A.M. Alkilany, C.J. Murphy, Toxicity and cellular uptake of gold nanoparticles: what we have learned so far?, J. Nanopart. Res., 12 (2010) 2313-2333.
[22] P. Rivera Gil, G. Oberdörster, A. Elder, V. Puntes, W.J. Parak, Correlating Physico-Chemical with Toxicological Properties of Nanoparticles: The Present and the Future, ACS Nano, 4 (2010) 5527-5531.
[23] G. Maiorano, S. Sabella, B. Sorce, V. Brunetti, M.A. Malvindi, R. Cingolani, P.P. Pompa, Effects of Cell Culture Media on the Dynamic Formation of Protein−Nanoparticle Complexes and Influence on the Cellular Response, ACS Nano, 4 (2010) 7481-7491.
[24] E. Sabbioni, S. Fortaner, M. Farina, R. Del Torchio, C. Petrarca, G. Bernardini, R. Mariani-Costantini, S. Perconti, L. Di Giampaolo, R. Gornati, M. Di Gioacchino, Interaction with culture medium components, cellular uptake and intracellular distribution of cobalt nanoparticles, microparticles and ions in Balb/3T3 mouse fibroblasts, Nanotoxicology, 8 (2014) 88-99.
[25] R. Miller, V.B. Fainerman, A.V. Makievski, J. Krägel, D.O. Grigoriev, V.N. Kazakov, O.V. Sinyachenko, Dynamics of protein and mixed protein/surfactant adsorption layers at the water/fluid interface, Adv. Colloid Interface Sci., 86 (2000) 39-82.
[26] C.L. Dora, L.F.C. Silva, J.L. Putaux, Y. Nishiyanna, I. Pignot-Paintrand, R. Borsali, E. Lemos-Senna, Poly(ethylene glycol) hydroxystearate-based nanosized emulsions: effect of surfactant concentration on their formation and ability to solubilize quercetin, J Biomed Nanotechnol, 8 (2012) 1-9.
[27] A. Verma, F. Stellacci, Effect of Surface Properties on Nanoparticle–Cell Interactions, Small, 6 (2010) 12-21.
[28] E.C. Cho, J. Xie, P.A. Wurm, Y. Xia, Understanding the Role of Surface Charges in Cellular Adsorption versus Internalization by Selectively Removing Gold Nanoparticles on the Cell Surface with a I2/KI Etchant, Nano Lett., 9 (2009) 1080-1084.
[29] P.V. Khachane, A.S. Jain, V.V. Dhawan, G.V. Joshi, A.A. Date, R. Mulherkar, M.S. Nagarsenker, Cationic nanoemulsions as potential carriers for intracellular delivery, Saudi Pharm. J., 23 (2015) 188-194.
[30] Y. Hu, T. Litwin, A.R. Nagaraja, B. Kwong, J. Katz, N. Watson, D.J. Irvine, Cytosolic delivery of membrane-impermeable molecules in dendritic cells using pH-responsive core-shell nanoparticles, Nano Lett., 7 (2007) 3056-3064.
[31] F. Afaq, Natural agents: Cellular and molecular mechanisms of photoprotection, Arch. Biochem. Biophys., 508 (2011) 144-151.
[32] S. Arora, J.M. Rajwade, K.M. Paknikar, Nanotoxicology and in vitro studies: The need of the hour, Toxicol. Appl. Pharmacol., 258 (2012) 151-165.

[33] Z. Magdolenova, A. Collins, A. Kumar, A. Dhawan, V. Stone, M. Dusinska, Mechanisms of genotoxicity. A review of in vitro and in vivo studies with engineered nanoparticles, Nanotoxicology, 8 (2014) 233-278.
[34] F. Afaq, M.A. Zaid, N. Khan, M. Dreher, H. Mukhtar, Protective effect of pomegranate-derived products on UVB-mediated damage in human reconstituted skin, Exp. Dermatol., 18 (2009) 553-561.
[35] L.A. Pacheco-Palencia, G. Noratto, L. Hingorani, S.T. Talcott, S.U. Mertens-Talcott, Protective Effects of Standardized Pomegranate (Punica granatum L.) Polyphenolic Extract in Ultraviolet-Irradiated Human Skin Fibroblasts, J Agric Food Chem, 56 (2008) 8434-8441.
[36] D.N. Syed, A. Malik, N. Hadi, S. Sarfaraz, F. Afaq, H. Mukhtar, Photochemopreventive Effect of Pomegranate Fruit Extract on UVA-mediated Activation of Cellular Pathways in Normal Human Epidermal Keratinocytes, Photochem Photobiol, 82 (2006) 398-405.
[37] M.A. Zaid, F. Afaq, D.N. Syed, M. Dreher, H. Mukhtar, Inhibition of UVB-mediated oxidative stress and markers of photoaging in immortalized HaCaT keratinocytes bu pomegranate polyphenol extract POMx, Photochem Photobiol, 83 (2007) 882-888.
[38] S. Kondo, T. Kono, D.N. Sauder, R.C. McKenzie, IL-8 gene expression and production in human keratinocytes and their modulation by UVB, J. Invest. Dermatol., 101 (1993) 690-694.
[39] I. Strickland, L.E. Rhodes, B.F. Flanagan, P.S. Friedmann, TNF-alpha and IL-8 are upregulated in the epidermis of normal human skin after UVB exposure: Correlation with neutrophil accumulation and E-Selectin expression, J. Invest. Dermatol., 108 (1997) 763-768.
[40] T. Welss, D.A. Basketter, K.R. Schröder, In vitro skin irritation: facts and future. State of the art review of mechanisms and models, Toxicology in Vitro, 18 (2004) 231-243.
[41] A. Storey, F. McArdle, P.S. Friedmann, M.J. Jackson, L.E. Rhodes, Eicosapentaenoic Acid and Docosahexaenoic Acid Reduce UVB- and TNF-[alpha]-induced IL-8 Secretion in Keratinocytes and UVB-induced IL-8 in Fibroblasts, J Investig Dermatol, 124 (2004) 248-255.
[42] N. Di Girolamo, R.K. kUMAR, M.T. Coroneo, D. Wakefield, UVB-mediated induction of interleukim-6 and -8 in pterygia and culture human pterygium epithelial cells, Investigative Ophthalmology & Visual Science, 43 (2002) 3430-3437.
[43] E.A. Dutra, D.A.G.C. Oliveira, E.R.M. Kedor-Hackmann, M.I.R.M. Santoro, Determination of sun protection factor (SPF) of sunscreens by ultraviolet spectrophotometry, Brazilian Journal of Pharmaceutical Science, 40 (2004) 381-385.
[44] S. El-Boury, C. Couteau, L. Boulande, E. Paparis, L.J.M. Coiffard, Effect of the combination of organic and inorganic filters on the Sun Protection Factor (SPF) determined by in vitro method, International Journal of Pharmaceutics, 340 (2007) 1-5.
[45] A. Jarzycka, A. Lewinska, R. Gancarz, K.A. Wilk, Assessment of extracts of Helichrysum arenarium, Crataegus monogyna, Sambucus nigra in photoprotective UVA and UVB; photostability in cosmetic emulsions, J. Photochem. Photobiol., B, 128 (2013) 50-57.
[46] C.D. Kaur, S. Saraf, Photochemoprotective activity of alcoholic extract of *Camellia sinensis*, International Journal of Pharmacology, 7 (2011) 400-404.
[47] A.C.V. Mota, Z.M.F. Freitas, E. Ricci Júnior, G.M. Dellamora-Ortiz, R. Santos-Oliveira, R.A. Ozzetti, A.L. Vergnanini, V.L. Ribeiro, R.S. Silva, E.P. Santos, In vivo and in vitro evaluation of octyl methoxycinnamate liposomes, International Journal of Nanomedicine, 8 (2013) 4689-4701.

[48] P.S. Wu, L.N. Huang, Y.C. Guo, C.C. Lin, Effects of the novel poly(methyl methacrylate) (PMMA)-encapsulated organic ultraviolet (UV) filters on the UV absorbance and in vitro sun protection factor (SPF), J. Photochem. Photobiol., B, 131 (2014) 24-30.
[49] Y. Seto, K. Hosoi, H. Takagi, K. Nakamura, H. Kojima, S. Yamada, S. Onoue, Exploratory and regulatory assessments on photosafety of new drug entities, Current Drug Safety, 7 (2012) 140-148.
[50] A.W. Girotti, Photosensitized oxidation of membrane lipids: reaction pathways, cytotoxic effects, and cytoprotective mechanisms, J. Photochem. Photobiol., B, 63 (2001) 103-113.
[51] A.A. Schothorst, J. Van Steveninck, L.N. Went, D. Suurmond, Photodynamic damage of the erythrocyte membrane caused by protoporphyrin in protoporphyria and in normal red blood cells, Clinica Chimica Acta, 39 (1972) 161-170.
[52] OECD, OECD Guidelines for the Testing of Chemicals Test No. 432: In Vitro 3T3 NRU Phototoxicity Test, (2004).